6 Voltage-Gated Sodium Channels

Dorothy A. Hanck and Harry A. Fozzard

6.1 Introduction

Voltage-gated sodium channels subserve regenerative excitation throughout the nervous system, as well as in skeletal and cardiac muscle. This excitation results from a voltage-dependent mechanism that increases regeneratively and selectively the sodium conductance of the channel e-fold for a 4–7 mV depolarization of the membrane with time constants in the range of tens of microseconds. Entry of Na^+ into the cell without a companion anion depolarizes the cell. This depolarization, called the action potential, is propagated at rates of 1–20 ms^{-1}. In nerve it subserves rapid transmission of information, and in muscle cells, coordinates the trigger for contraction. Sodium-dependent action potentials depolarize the membrane to inside positive values of about 30–40 mV (approaching the electrochemical potential for the transmembrane sodium gradient). Repolarization to the resting potential (usually between -60 and -90 mV) occurs because of inactivation (closure) of sodium channels, which is assisted in different tissues by variable amounts of activation of voltage-gated potassium channels. This sequence results in all-or-nothing action potentials in nerve and fast skeletal muscle of 1–2 ms duration, and in heart muscle of 100–300 ms duration. Recovery of regenerative excitation, i.e., recovery of the ability of sodium channels to open, occurs after restoration of the resting potential with time constants of a few to several hundreds of milliseconds, depending on the channel isoform, and this rate controls the minimum interval for repetitive action potentials (absolute refractory period).

The sodium channel that is responsible for this complex time- and voltage-dependent behavior is an integral membrane protein of greater than 200 kDa; it spans the cell's surface membrane with a large mass located both intracellularly and extracellularly. Five structural properties underlie the complex channel function described above: (1) the pore or permeation path, which connects the outside and inside salt solutions, (2) the narrowest region of the pore, which determines the selectivity for sodium over other physiologically present cations, (3) the gates, which open or shut the channel, i.e., control activation and inactivation, (4) the process that couples the gates to transmembrane voltage, and (5) the various binding sites that allow the modulation of the channel by drugs and natural toxins. Various clinical diseases of the nervous system and muscle result from subtle changes in the channel's structure and consequent function.

Dorothy A. Hanck and Harry A. Fozzard

This chapter will describe the protein, the permeation path and its selectivity property, the gates and their control by membrane voltage, and some of the changes that result in human disease. The crucial and remarkable ability of these voltage-dependent channels to monitor transmembrane voltage has been thoroughly discussed by Francisco Bezanilla in his chapter in this volume, and we will discuss only features that are specific for the sodium channel.

The channel protein (∀-subunit) is large, i.e., about 2000 amino acids. It is organized into four homologous and covalently linked domains, each resembling one subunit of the potassium channel. Some isoforms are found together with smaller ∃-subunits, which are single membrane-spanning subunits that modulate membrane expression and channel function. However, all of the essential elements of the channel seem to be accounted for by the ∀-subunit. The water-filled cation permeation path, the pore, has been located by interaction with several natural toxins and clinically used drugs. Its narrowest region is responsible for close interaction with the permeating cation, selecting sodium for permeation over all other ions physiologically present. The pore can be occluded by two gates. The activation gate, which is generally thought to lie near the inside mouth of the pore, opens in response to depolarization by coupling with part of the voltage sensor. A intracellular segment is drawn into the pore after opening; blocking permeation. The speed of this process, called fast inactivation, is coupled to the position of voltage sensors. Additional slower processes can also occlude the pore, a process called slow inactivation. Most diseases associated with sodium channel abnormalities are gain-of-function, although rarer loss of function mutants have also been described, which are associated with sudden cardiac death, usually from a reduction in functional channels. Obviously, loss of all sodium channels in mammalian cells is embryonically lethal. Little direct structural information is available for this large complex protein. However, the opportunity to work with cloned sodium channels expressed in heterologous cells has been a key to relating structure to function in this protein. We also benefit by analogy from insights gained from studies of other cation channel types.

6.2 The Sodium Channel as a Protein

The channel is a large, glycosylated, intrinsic membrane protein. Its primary α-subunit is usually greater than 2000 amino acids long, and this subunit forms the functional unit of the channel (Fozzard and Hanck, 1996; Catterall, 2000). Some sodium channel isoforms in some tissues are expressed with additional smaller subunits (β-subunits), which affect gating kinetics and membrane expression levels. It is possible to identify four highly homologous regions of the α-subunit that appear to form four covalently linked intramembrane domains. Each of the domains (I–IV) includes six α-helical segments that are long enough to cross the membrane (S1–S6). In addition to being similar to each other, the four domains are similar to the six-helix mammalian potassium channel subunit, four of which can assemble to form a channel. The long N- and C-termini of the protein and the three linkers between the

four transmembrane domains are intracellular and they are not as homologous. Thus, the α-subunit is a four-domain protein with 24 transmembrane α-helices, organized circumferentially around a central pore. About half of the protein is intracellular, a third is intramembrane, and a sixth is extracellular.

Nine isoforms of mammalian channels have been found so far (Goldin, 2001). Three (Nav1.1, Nav1.2, and Nav1.3) are found in the central nervous system, three are in the peripheral nervous system (Nav1.7, Nav1.8, and Nav1.9), and one (Nav1.6) is seen in both regions. Nav1.4 is exclusively in skeletal muscle, and Nav1.5 is mainly in the heart, but also has been found in the central nervous system. These isoforms are 80–90% identical, but have markedly different gating kinetics and drug/toxin interactions. Many other sodium channel genes have been sequenced from nonmammalian tissues, but only the insect isoform has been expressed and studied.

Similar to the potassium channel subunit, each domain contains one α-helical segment (S4) that contains multiple positively charged residues, located at three-residue intervals, and that are responsible for voltage-sensing (Bezanilla, 2000). The S5 and S6 segments of each of the four domain form the lining of the centrally located pore, with their extracellular connecting segments (P loops) folded back into the membrane to form the pore's outer vestibule. The domains are arranged around the pore in a clockwise pattern, when viewed from the outside (Dudley et al., 2000). Thus, the intramembrane part of each domain has a voltage-sensing part—the S1–S4, and a pore-forming part, the S5-P-S6.

No X-ray crystal structures have been obtained of the sodium channel α-subunit, and its size and hydrophobicity suggest that such information will not soon be available. However, its homology to the potassium channel intramembrane component, which has been crystalized, has allowed some inference as to the three-dimensional structure of that part of the protein. Pieces of the cytoplasmic regions have been structurally defined (see later). Crystalization has been successful for several bacterial channels, and a particularly interesting gene (NaChBac) has been isolated from a bacterium. It has significant homology to one domain of the mammalian channel, and expression of this bacterial gene yields a channel that is sodium selective (Ren et al., 2001).

6.3 The Pore

6.3.1 General Strategy

Ions transit the channel by diffusion down an electrochemical gradient through a water-filled path that is created by the protein structure. Although the physiological gradients are such that normally Na^+ diffuses into the cell, experimental conditions can be altered to reverse the flow. The pore is located between the intramembranous parts of the four domains. It is able to discriminate between ions as similar as $Na^+$and K^+, so it must remove some of the ions' waters of hydration, allowing

direct interaction between the protein and the ion. Removal of waters of hydration would require excessive energy without surrogate interactions between the ions and the pore wall. Consequently, at least some part of the pore must be narrow enough for its walls to interact directly with ions with an unhydrated radius of $\sim$1 Δ or partially dehydrated ions. For our discussion, the pore will be divided into four parts: the outer vestibule, the selectivity ring, the inner pore, and the gating region.

The original definition of the pore was made with biophysical tools—measurements of currents carried by different ions in response to voltage changes. Since the channel has been cloned and subject to expression in cells with little or no voltage-dependent currents, chimerae and point mutations of these channels have been prime tools for unraveling the relationship between structure and function.

In nature there are a number of toxins that target the sodium channel, producing block or changes in gating kinetics (Catterall, 1980). These toxins were crucial in the biochemical purification necessary for the original channel cloning by providing tags to trace the channel in broken membrane fractions, where its characteristic electrical properties could not be measured. Some of the toxins bind with high affinity to specific sites. Two classes that have been important in resolving the pore are the guanidinium toxins, tetrodotoxin (TTX) and saxitoxin (STX), and the μ-conotoxins (μ-CTX). TTX is found mainly in organs of the pufferfish, a culinary delicacy in Japan. STX is the toxin in Red Tide. They are small, compact, and charged molecules that are only somewhat larger than hydrated sodium ions. μ-CTX is a 22-amino acid peptide that is used by the Conus snails to paralyze their prey (French and Dudley, 1999). In addition, a commonly used drug class—local anesthetics (LA)—also target the sodium channel and have been useful in defining the region of their binding.

6.3.2 Outer Vestibule

Shortly after cloning of several isoforms a stretch of amino acid residues in each extracellular connecting segment between each domain's S5 and S6 that is highly conserved across all sodium channel isoforms was predicted to be the region that might determine selectivity (Guy and Seetharamulu, 1986). On the basis of hydrophobicity and secondary structural preferences of the segment they proposed that it folded back into the membrane as a helix-strand hairpin. Because of the circumferential location of the domains, these four "P loops" then could form the outer entrance to the pore. This fourfold P-loop pattern aligned a perfectly conserved ring of amino acid residues at the innermost extent of the hairpin—aspartate, glutamate, lysine, and alanine for domains I to IV, respectively (DEKA motif), and this was proposed to contribute to the sodium selectivity of the channel (see later). Three or four residues distal (toward the C-terminus) from the putative selectivity ring was another perfectly conserved ring of carboxylates—glutamate, glutamate, aspartate, and aspartate, although its critical function was not clear at the time. Noda and colleagues found that neutralization of the glutamate in this domain I outer ring greatly diminished TTX block (Noda et al., 1989), and this finding was expanded to include the other charged ring residues (Terlau et al., 1991). This work confirmed that these

P-loops were part of the TTX binding site and likely to be the outer pore mouth. The cardiac isoform of the sodium channel (Nav1.5) is known to be dramatically less sensitive to TTX block, but only two residues in the lining of the putative outer vestibule are different. Studies of point mutations of these residues showed that the TTX sensitivity differences resulted from the amino acid difference just C-terminus to the domain I selectivity ring aspartate. Cysteine, found in this position in Nav1.5, conferred resistance to TTX (Satin et al., 1992), while tyrosine in Nav1.4 (Backx et al., 1992) or phenylalanine in Nav1.2 (Heinemann et al., 1992) was associated with sensitivity. Subsequently, Nav1.6, with a serine in this position, was found to be resistant. Lipkind and Fozzard (1994) modeled the vestibule by assembling the P-loops to form a coherent binding site for TTX and measured its predicted binding interactions. They found that the aromatic residue in domain I P-loop provided a hydrophobic interaction with TTX that added about -4 kcal mol^{-1} of interaction energy, accounting for the high affinity state. Subsequently, Penzotti et al. (2001) determined the change in TTX-channel interaction energy with mutation of the other critical vestibule residues matched that predicted by the Lipkind–Fozzard model, supporting the model as a reasonable approximation of the conformation of the outer vestibule.

The snail toxin μ-conotoxin (μ-CTX) competes with TTX binding, so their binding sites are likely to overlap. Because μ-CTX is a small peptide, analogs could be synthesized with changes in individual amino acid residues, in order to determine their roles in the toxin-channel binding interaction (Becker et al., 1992). Arg-13 was found to play the largest role in μ-CTX binding energy, and mutant cycle analysis was consistent with the critical interaction of Arg-13 being with the domain II outer ring glutamate (Chang et al., 1998). However, modeling the interaction suggested that the toxin bound eccentrically in the pore and failed to occlude it. Careful study indicated that part of the blocking mechanism of Arg-13 and μ-CTX was electrostatic repulsion of sodium ions by the critically located positive charge of Arg-13 (Hui et al., 2002), rather than simple steric occlusion of the pore. In summary, interaction of the guanidinium toxins and μ-CTX with the channel created a consistent structural picture of the outer vestibule as a shallow funnel about 10 Δ in diameter at the outside negatively charged ring, which tapers to a 3 × 5 Δ selectivity ring. Its volume is sufficient for 30–40 water molecules, forming a constrained hydrophilic environment above the selectivity filter.

6.3.3 Selectivity

The channel discriminates between Na^+ and K^+ with a permeability ratio of $>10{:}1$, with a permeation rate under standard conditions of about 10 million Na^+ per second. The radius of Na^+ is 0.95 Δ and the radius of K^+ is 1.33 Δ, depending on the method of its measurement. Both have a single unit positive charge and are hydrated, with energies of -105 and of 85 kcal mol^{-1}, respectively. When hydrated, these ions are almost indistinguishable, so it was realized quite early that at least partial dehydration of the ions would be required, if they were to be identified, so that only Na^+ is allowed

to permeate. However, the energies required for dehydration are huge, and there was no straightforward way for the channel to accomplish this and still allow a permeation rate of 10 million ions per second (maximal transit time of 100 ns). It seemed plausible that some component of the channel pore be able to contribute equivalent energy to the water of hydration and still permit the rapid ion transit. Therefore, it was suggested that the pore protein lining could substitute energetically for water. Since Na^+ has a higher energy of hydration than K^+, the oxygen in a carboxylate group is more likely than the lower energy of the oxygen of a carbonyl or hydroxyl group to interact with Na^+(and visa versa for K^+).

The DEKA inner ring of the vestibule formed by the P-loops has two such carboxylates, with an adjacent lysine. The glutamate in domain II and lysine in domain III were critical for Na:K selectivity, and the lysine (or arginine) was necessary to block Ca permeation (Favre et al., 1996; Schlief et al., 1996). Favre et al. suggested that in the selectivity ring the lysine acts as a tethered cation, blocking interaction of cations with the carboxylates, and Na^+ is energetically able to move it away (Lipkind and Fozzard, 2000). The lysine also lowers binding affinity of Na^+ for the selectivity filter, favoring dissociation and rapid permeation (Fig. 6.1).

The influence of the outer ring carboxylates on selectivity is small, but they play a large role in permeation rate (Terlau et al., 1991). One possible clue to the outer ring function is that the sodium current is quite sensitive to pH in the physiological range. The current can be titrated by acid solutions with single site pKa values of about 6. Free aspartate and glutamate have pKa values of 4.0–4.5, but this is shifted markedly in the alkaline direction in a negative field. The outer ring carboxylates do create a strong negative field in the vestibule, shifting pKa values of the amino acids in the vestibule lining into the physiological range. Because of the single site titration curve, they appear to create a single site in the vestibule that may contribute to the dehydration process (Schild and Moczydlowski, 1994; Khan et al., 2002). If these carboxylates are neutralized by protons at low pH, the field is reduced and they are less effective in dehydration of Na^+, reducing the single-channel conductance. The calculated field in the vestibule was -58 to -93 mV. For comparison, Hui et al. (2002) titrated a histidine mutant of μ-CTX in the pore and estimated that the vestibule potential was at least -100 mV.

6.3.4 Inner Pore Gates

Sodium channels have at least two structures that gate the channel open or closed. The activation gate is opened within microseconds by depolarization and consequent movement of the S4 voltage sensors. A fast inactivation gate then shuts, partly related to depolarization-induced movement of the S4 voltage sensors and partly related to the open conformation of the activation gate (see later). There are several slower inactivation processes that are less well understood and may result from collapse of some part of the pore.

The crystalization of a bacterial potassium channel (Doyle et al., 1998) predicts a general structure for the pore of ion selective channels. The KcsA crystal structure

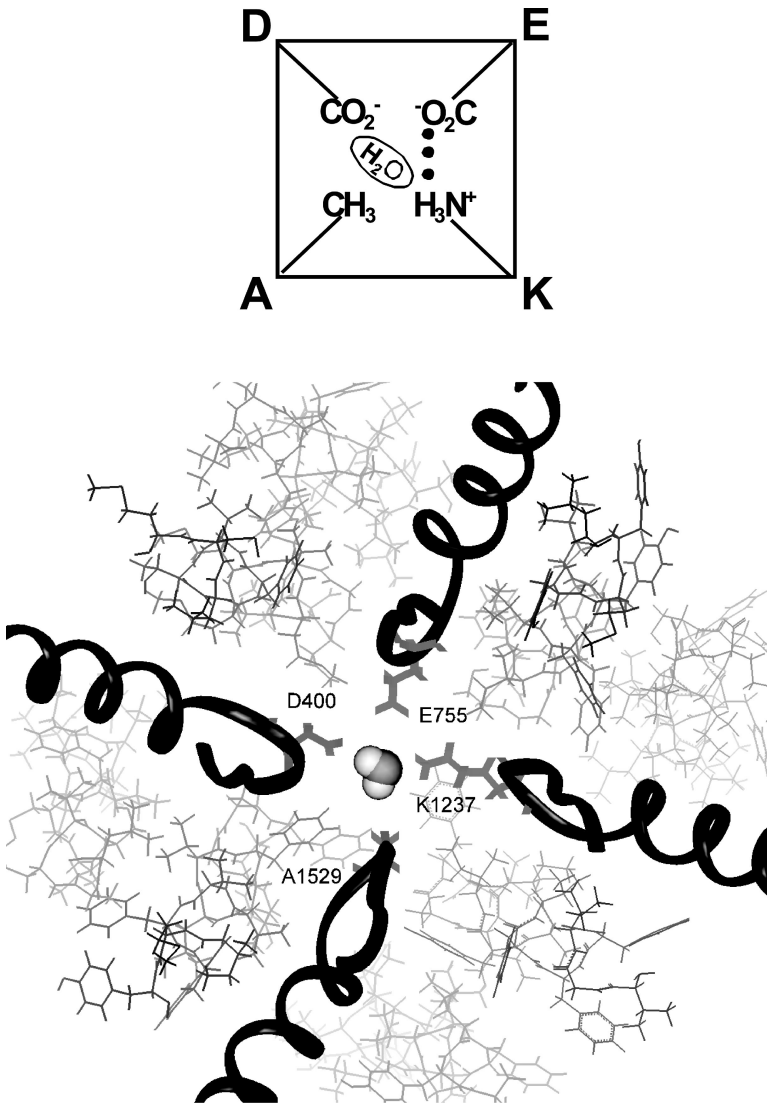

Fig. 6.1 The selectivity filter of the Na channel (using sequence of μ1) with residues of the DEKA motif shown schematically (A) and by space-filling images (B). The side chains of Glu-755 and Lys-1237 of domains II and III are located at a distance compatible with a salt bridge interaction. The side chains of Asp-400 of domain I and Lys-1237 are separated by one molecule of water, which is shown in the center of the figure. The open area inside the pore is about 3 × 5 Δ (in the absence of water), and there is room for the side chain of Lys-1237 to more toward Ala-1529. DEKA (Asp-400, Glu-755, Lys-1237, and Ala-1529) are located in the turns of P-loops of domain I–IV, which are shown by ribbons. The space between the P-loops is filled by S5 and S6 ∀-helices. This arrangement is based on available mutagenesis data and binding data for TTX and STX (Lipkind and Fozzard, 2000).

shows that the S5-P-S6 components of each domain cross the membrane at an angle, overlapping near the inside. This "teepee" structure of the KcsA channel is characteristic of a closed channel. Comparison with the crystal structure of the open MthK channel (Jiang et al., 2002) shows that for an open channel the S6 helices are bent at glycine residues and the inner halves are hinged away from the pore. Using a similar orientation of the S6 helices of the sodium channel, Sunami et al. (2004) found that the mutants F1579C and V1583C of IVS6, residues predicted to be located just below the selectivity filter were accessible to the hydrophilic, positively charged, MTSET from the inside, only if the activation gate was opened, placing the activation gate at the S6 crossover (Lipkind and Fozzard, 2000). The location of the S6 activation hinge is not entirely clear yet. For MthK the hinges were glycine residues, and for the Shaker potassium channel it is probably a proline-x-proline. The sodium channel S6 segments have no prolines and in place of a glycine in domain IV there is a serine. Using serines and glycines as hinges Lipkind and Fozzard (2005) were able to model an open pore for the sodium channel.

6.4 Gating

Prior to the molecular cloning of channels, our understanding of how voltage controls gating was almost exclusively derived from investigation of voltage-gated sodium channels in a few model organisms where channel expression was particularly high, e.g., squid giant axon. After cloning, however, potassium channels became the most common channel-type used for gating studies. DNAs were <2 kb rather than the >6 kb for sodium channels, since potassium channels could be expressed with four identical subunits rather than as a single polypeptide with four connected, nonidentical pseudo-domains. Not only is it easier to work with smaller DNAs, but it was reasonable to assume that expressed channels would be fourfold symmetric, and introduced amino acid changes would yield four substitutions per channel. Potassium channels, especially Shaker delta (amino acids 4–46 deleted, which removed the fast inactivation particle) expressed well, and the clones were freely shared in the research community. Consequently, they became the standard for studies of voltage gating. The advantage of multiple investigators working on the same isoform, often expressed in the same background (usually *Xenopus* oocytes) was a boon to biophysical investigations because time need not be spent considering isoform or background and experimental differences, and investigators could build on each others' results. Such studies, in combination with the crystallization of a voltage-gated bacterial channel, has produced a fairly detailed, although not yet complete, understanding of how voltage controls opening (activation) of voltage-gated channels. The reader is directed to the discussion of gating by Bezanilla in this volume, which focuses on activation gating largely derived from studies of these potassium channels.

Voltage-dependent sodium channels are more complicated than potassium channels because the sodium channels have four pseudo-domains coded by a single

DNA, which produces channels with four nonidentical gating structures. Simple inspection suggests that either each domain contributes to all gating processes, or more intriguingly, that domains have differentiated to become important for different aspects of gating. In fact the first structure–function studies of sodium channels (Stuhmer et al., 1989), which are principally remembered because they were the first the establish the role of S4 positive charges as the voltage sensor, also reported experiments in which DNA was cut in a region predicted to be in the intracellular linker between domains III and IV, producing channels that inactivated poorly. At the time the suggestion was made that the Hodgkin–Huxley description of sodium channel gating as m^3h (Hodgkin and Huxley, 1952) might arise because the S4s in domains I, II, and III accounted for activation while the S4 of domain IV controlled inactivation. This would contrast with potassium channels, where activation was described as n^4, with all four voltage sensors contributing to activation.

To understand why the idea of identifying the S4 segments with the Hodgkin–Huxley probability factors was not immediately seized upon with enthusiasm, one needs to consider several earlier studies beginning with the development of gating charge measurement techniques in the 1970s. Gating currents represent the membrane delimited movement of the S4 charged amino acids in response to changes in membrane potential. The suggestion by the Hodgkin–Huxley analysis that inactivation was a single, voltage-dependent process that proceeded similarly from all closed states as well as the open state (h) was one of the important predictions that could be addressed by experiments measuring gating currents. In a landmark paper, Armstrong and Bezanilla (1977) established that a voltage dependence of inactivation could not be directly demonstrated. Rather inactivation could be appreciated only by a slow time-dependence of the recovery of activation charge, a process they described as charge immobilization. Other experimenters confirmed these results, leading to the idea that inactivation was independent of voltage, and its apparent voltage dependence arose because it was linked to voltage-dependent activation. Experimental data in sodium channels also supported the idea that voltage sensing was not the coordinated movement of identical voltage sensors (independence of gating). This meant that m^3h was a useful formalism for model calculations, but actual activation gating proceeded as a complex process with different amounts of gating charge in each step.

Recording of single channel activity made it possible for the first time to obtain direct estimation of channel gating transition rate constants. Aldrich, Corey, and Stevens recorded single-channel events of sodium channels in mammalian neuroblastoma cells, observing that mean open time was much shorter than the decay of the macroscopic current and was voltage independent over a large voltage range (Aldrich et al., 1983). They concluded, therefore, that inactivation from the open state was essentially voltage independent and the voltage dependence of macroscopic current decay arose not from a voltage-dependent inactivation process but from the distributed arrival of channels at the open state, i.e., the voltage dependence of activation. Based on these 1983 experiments and those they published later (Aldrich and Stevens, 1987), in combination with the available gating current data,

the idea that inactivation was itself a voltage-independent process became accepted as axiomatic. When single-channel recordings were finally achieved in squid giant axon, Vandenberg and Bezanilla (1991) also described inactivation from the open state as voltage independent, although they required the I–O transition to be voltage dependent.

After heterologous expression of cloned sodium channels became available, mutagenesis studies in the early 90s led to the identification of a stretch of residues in the intracellular linker between domains III and IV that needed to be hydrophobic in order for inactivation from the open state to occur. The IFM motif (West et al., 1992) was supported experimentally by other similar experiments of the time, and the idea that this region of the channel bound and occluded permeation, acting as a hinged lid (Catterall, 2000), became accepted. The similarity between these data in sodium channels and the ball and chain motif identified by the Aldrich laboratory in the N-terminus of the Shaker potassium channel (Hoshi et al., 1990), where decay of the current and fast inactivation was essentially voltage independent, comfortably supported the gating current data of the late 70s and the single channel data in mammalian neuronal cells. The IFM peptide has been characterized structurally by NMR, showing a hydrophobic core hinged to an ∀-helical segment (Rohl et al., 1999; Kuroda et al., 2000).

In this same time period, however, several laboratories reported single-channel data for the isoform of sodium channels found in native cardiac cells. Each of these (Berman et al., 1989; Yue et al., 1989; Scanley et al., 1990) observed a biphasic dependence of channel mean open time on voltage, suggesting that inactivation from the open state might be voltage dependent in some sodium channel isoforms.

Before cloning, biophysical investigation of channels was restricted to a few cell types in which expression was particularly high. Mammalian preparations were, in general, not suitable for gating current studies. After development of techniques for the isolation of single cells from mammalian tissues, a number of cardiac preparations were found to express a high density of sodium currents, with Purkinje cells in the conduction system of the heart having a particularly high expression level (Makielski et al., 1987). Development of a large bore pipette made from theta glass allowed for recording from canine Purkinje cells with high fidelity, as well as the ability to change intracellular solutions. Using this recording method, it was possible to observe directly the gating charge of sodium channels as a nonlinear signal that added to the linear charge needed to establish voltage across the cell membrane in these cells (Hanck et al., 1990) (Fig. 6.2).

Gating charge for this cardiac isoform resembled that previously observed for other sodium channels with the exception that rather than moving over a more negative potential range than channels activated, it was quite similar to activation (Fig. 6.3) suggesting a tighter relationship of charge movement to the opening transition than for other sodium channels (Sheets and Hanck, 1999). But it was the use of a toxin that produced insight into whether inactivation was fundamentally different in this

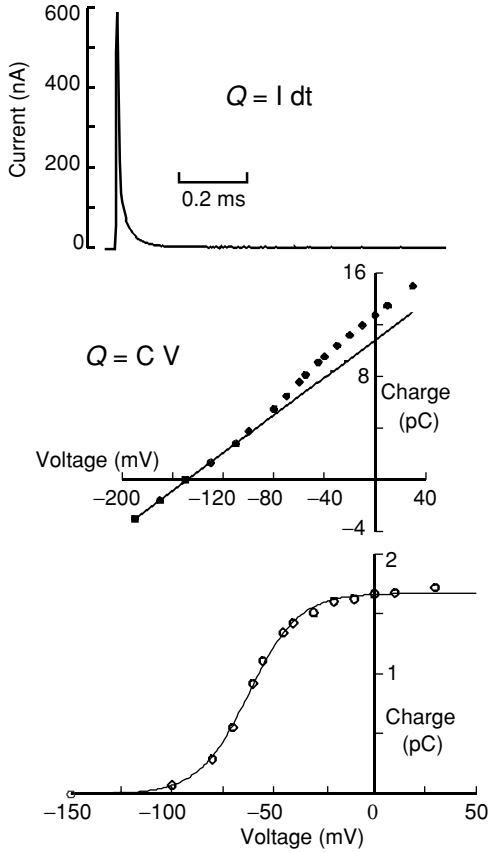

Fig. 6.2 Recording of linear and nonlinear components of capacitive currents. Upper panel shows raw currents recorded from a cardiac Purkinje cell in response to a 40 mV step from −150 mV to −110 mV. Middle panel shows total charge as a function of voltage for a series of steps in which all ionic current was eliminated by replacement of sodium with TMA and addition of 10:M STX. Line is the best fit to data between −100 and −200 mV and represents the charging of the membrane, capacitance of this cell was 73 pF. Lower panel shows the nonlinear charge (gating charge) calculated as the difference between total charge and the linear component.

isoform. As we have noted, toxins have been important molecules for the understanding of ion channels. Certainly, the use of TTX for selective block of sodium channels is well appreciated (see earlier). Investigators searched for additional channel-specific toxins, and in the 80s the Catterall laboratory was particularly successful at discovering and characterizing toxins that produced a variety of kinetic effects (Catterall, 1980). Members of one class of toxins that was of interest in the cardiac field were the site 3 toxins. Although of diverse origin and molecular weight (isolated from both scorpions and sea anemone) they shared the property of sparing activation and selectively inhibiting inactivation in the neuronal preparations in

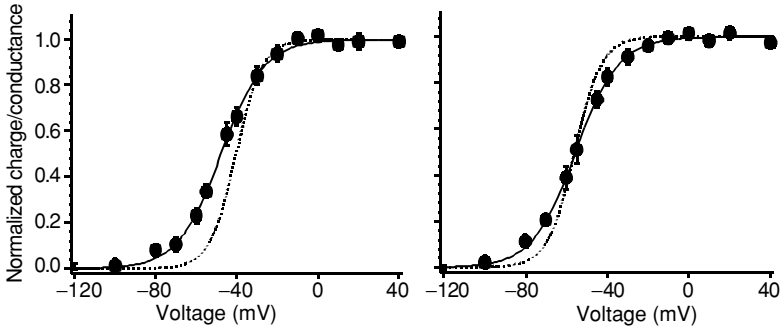

Fig. 6.3 Superimposed peak charge–voltage (!) and conductance–voltage (dotted line) relationships for rSkM1 (:1) sodium channels (left) and for hH1a Na channels (right). Note that for :1 charge–voltage relationship is largely to the left of the conductance–voltage relationship whereas for the cardiac isoform the charge–voltage and conductance–voltage relationships are superimposed. Redrawn from Sheets and Hanck (1999).

which they had been studied. One of these, Anthropleura A, which was isolated from the giant green sea anemone found broadly in the pacific coastal tidepools (ApA), is particularly effective in the heart (Hanck and Sheets, 1995; Sheets and Hanck, 1995).

In voltage clamp experiments ApA indeed did not affect the time course of the onset of the current, the time course of tail currents at negative potentials (when the primary transition was channel closure from the open state), or the midpoint of activation. Instead it markedly delayed current decay and, consistent with a selective effect on inactivation from the open state, was associated with a small increase in the rate of recovery of current at negative potentials and a marked slowing of recovery at positive potentials. With respect to gating charge ApA selectively reduced gating charge only at positive potentials, and difference charges (+/− toxin) showed a voltage dependence that was itself voltage dependent. This indicated inactivation from the open state was associated with charge movement rather than deriving its voltage dependence from channel activation (Hanck and Sheets, 1995; Sheets and Hanck, 1995). Interestingly, the toxin produced similar changes in gating in both cardiac and skeletal isoforms, consistent with a similar mechanism of action, albeit different affinity binding site, i.e., inhibition of movement of the domain IV voltage sensor (DIV/S4) (Sheets and Hanck, 1999). This suggests that domain IV S4 movement is tightly coupled to inactivation from the open state in all isoforms.

Additional mutagenesis experiments in $Na_V1.5$, combining S4 charge neutralizations with toxin modification, established that channel opening largely developed before the movement of DIV/S4, i.e., its movement was not required for channels to open (Sheets et al., 1999; Sheets et al., 2000). Movement of the domain IV voltage sensor was slow, and it was closely linked to prompt closure of the inactivation lid. The time course of movement of this charge was not affected by the presence or absence of the lid structure either during activation (on-gating charge) or during

repolarization (off-gating charge) (Sheets and Hanck, 2005). The conclusions of these experiments were confirmed by a second technique in which fluorescent markers were added to the channel. This fluorescent technique also demonstrated that the domain IV S4 charge moved slowly; in contrast, charge in domains I/S4 and II/S4 always moved rapidly. Domain III S4 resets slowly after hyperpolarization when fast inactivation is intact, so the presence of an intact lid retards charge recovery (immobilization).

Sodium channel recovery rates can vary significantly as a function of duration and frequency of depolarization, revealing multiple kinetically distinct components of channel inactivation. Although fast inactivation following brief and infrequent depolarization recovers in milliseconds, prolonged or repetitive depolarizations drive channels into more stable conformations from which recovery is on the order of seconds to minutes, a process termed "slow inactivation." Slow inactivation reduces cellular excitability during sustained depolarization caused, for example, by increased extracellular potassium, and during high-frequency bursts of action potentials in nerve and skeletal muscle resulting in their eventual termination. The extent of slow inactivation-induced alterations in excitability vary from tissue to tissue as a result of regional differences in action potential firing frequency and isoform-dependent differences in the extent of slow inactivation. Cardiac sodium channels, for example, do not slow inactivate as quickly or as completely as the skeletal muscle isoform (Richmond et al., 1998; O'Reilly et al., 1999), allowing for sustained firing of action potentials in cardiac tissue. In muscle, slow inactivation has been broken down further kinetically into several discrete components, called slow, intermediate, and ultra-slow. The process has been less well studied in nerve, where it is more difficult to separate discrete inactivation states and the time constants appear to be a continuum.

The structural and mechanistic details underlying slow inactivation, while not well understood, appear to be distinct from those controlling fast inactivation. Slow inactivation does not require prior development of fast inactivation as disruption of fast inactivation, either through intracellular application of proteolytic enzymes that degrade the DIII–IV linker or direct mutation of the IFM motif itself, does not abolish slow inactivation (Rudy, 1978; Cummins and Sigworth, 1996; Featherstone et al., 1996). In fact, removal of fast inactivation by mutation in the IFM motif increased the probability of channels entering the slow inactivated (Featherstone et al., 1996), suggesting that binding of the fast inactivation gate protects the channel from the conformational changes that underlie slow inactivation. Additionally, slow inactivation does not alter the binding and unbinding of the fast inactivation gate as measured by accessibility assays of the IFM motif, further supporting the idea that distinct gating mechanisms control fast and slow inactivation (Vedantham and Cannon, 1998).

A number of mutations altering slow inactivation have been identified but have yet to provide any clues as to the location of the slow inactivation gate(s). Although some mutations affecting slow inactivation have been found in the domain III–IV linker that contains the fast inactivation gate, others are widely scattered in the protein

and no pattern is yet apparent. Some of the first mutations modifying slow inactivation were found in Nav1.4 from individuals with hereditary muscle diseases (Barchi, 1997; Cannon, 2000). Others were serendipitous observations on mutations made for other reasons (Balser et al., 1996). At the very least, the identification of mutations that specifically alter slow inactivation gating provides potentially useful tools to probe structure–function questions relating to slow inactivation gating. Presumably, slow inactivation involves slow and extensive, albeit reversible, rearrangement of the protein. Pore collapse, akin to the conformational changes that occur in the pore during C-type inactivation of the potassium channel, has been suggested for slow inactivation of sodium channels. Several lines of evidence are consistent with the view that during slow inactivation the pore is occluded by dramatic rearrangements of the outer vestibule (Benitah et al., 1999; Todt et al., 1999; Ong et al., 2000; Struyk and Cannon, 2002; Xiong et al., 2003), the inner vestibule (Vedantham and Cannon, 2000; Sandtner et al., 2004), or the selectivity filter (Hilber et al., 2001, 2005). The slowing of entry into slow inactivated states by extracellular metals cations (Townsend and Horn, 1997) and a pore-binding toxin peptide (Todt et al., 1999) further supports the idea that a relationship exists between the pore and conformational changes associated with slow inactivation. Although the process is clearly voltage dependent, its relation to the S4 voltage sensors has not been resolved. In summary, the structural mechanism of slow inactivation is obscure at this time but it appears to be less focused and more complex than fast inactivation.

Changes in channel gating and conformational states not only affect excitability of the cells in which they are expressed, but also influence drug sensitivity. The sodium channel is the prime target for a large class of commonly used drugs—local anesthetics (LA). They are thought to block the sodium current by binding to the inner pore of the channel, with their affinity greatly enhanced by repetitive action potentials (use-dependence). Four residues located in the inner half of domain I, domain III, and IV S6 have been identified by mutation to contribute to the LA binding site. The most important are Phe-1764 and Tyr-1771 (Nav1.2) in domain IV S6, located two helical turns apart just below the selectivity filter and near the activation gate (Yarov-Yarovoy et al., 2002). A molecular model of the inner pore and LA binding site (Fig. 6.4) has been developed (Lipkind and Fozzard, 2005). This model is of an open channel based on the suggestion from crystal structure of the potassium channel MthK that the activation gate opens by hinging of S6 segments at glycine and serine residues located just below the filter (Jiang et al., 2002). A key feature of this model is that high affinity LA binding depends on the activated open conformation but not the fast inactivated state, consistent with evidence that this fast gate is not directly affected by LA binding (Vedantham and Cannon, 1999). The mechanism of block is not yet resolved, but is probably not simply steric. One plausible proposal is that LA binding stabilizes the slow inactivated conformation (for review, see Ulbricht, 2005). Alternatives include electrostatic block by the amino head of the LA molecule positioned in the inner pore (Lipkind and Fozzard, 2005) and stabilization of the domain III S4 in its depolarized position (Sheets and Hanck, 2003).

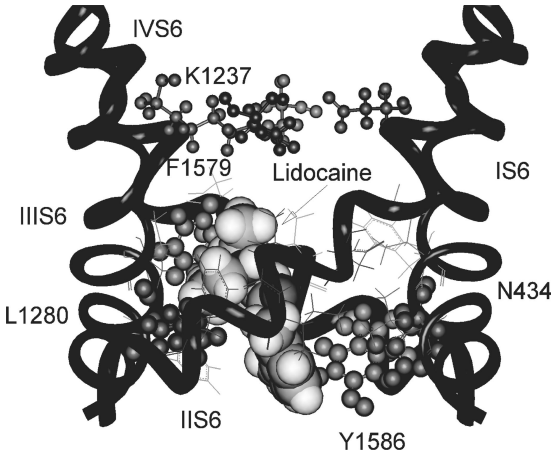

Fig. 6.4 Optimal location predicted for binding of lidocaine (shown as space filled) in the open pore of the Na channel (side view), using the μ1 Na channel sequence. The alkylamine head and the ethyl group at the linker bran produced the most optimal interactions with the side chains of Phe-1579 (DIV, S6) and Leu-1280 (DIII, S6). The dimethyl-substituted aromatic ring is in proximity to the side chain of Tyr-1586 (DIV, S6), which is adjacent to Asn-434 (DI, S6). The side chain of Phe-1579 forms the top of the binding site, and its location provides the most optimal interaction (van der Waals and electrostatic) with lidocaine. The amino acids that are predicted to make contact with lidocaine, based on available mutagenesis data, are shown as balls and sticks. Selectivity filter residues are also shown as balls and sticks in order to show the relationship of the predicted binding site to the selectivity filter. Based on the modeling of Lipkind and Fozzard (2005).

6.5 Hereditary Sodium Channel Diseases

Multiple polymorphisms have been found in the sodium channel gene, some rare and associated with high probability of disease and some common. The first sodium channel monogenic diseases were found in Nav1.4 (Cannon, 1996). Polymorphisms of Nav1.5 are found widely distributed in the population, and show some ethnic clustering (Makielski et al., 2003; Ackerman et al., 2004), and one of these seems to predispose to cardiac arrhythmia (Splawski et al., 2002). With the recent progress in genome-wide screening, it seems likely that differences in the sodium channel gene, in combination with other gene abnormalities or with environmental factors, will be found to be involved in variation in drug metabolism and in disease.

Monogenic skeletal muscle diseases include myotonias and periodic paralysis, depending on whether slow inactivation is enhanced (paralysis) or reduced (myotonia) (Cannon, 1996). The first cardiac mutation to be discovered results in one of the types of long QT syndrome—a highly lethal ventricular arrhythmia in young people (Wang et al., 1995). The mechanism of that mutation is disruption of the IFM inactivation motif. Subsequently, mutations in other locations have been found to cause long QT syndrome, especially ones in the proximal C-terminus.

Another closely related family of mutations have been associated with lethal ventricular arrhythmias in middle-aged persons (Brugada syndrome), and seem to be caused by a reduction in sodium channel expression (Chen et al., 1998). The main use for these discoveries of monogenic disease has been in diagnosis and prognosis, but directed therapy will develop in time. In the central nervous system polymorphisms have not been characterized as much. However, epilepsy associated with fevers has been associated with mutations in the ∃-subunit of the sodium channel (Wallace et al., 1998). These mutations not only identify disease mechanisms, but they also contribute indirectly to our understanding of the relation between structure and function of the normal sodium channel.

Acknowledgments

We thank Gregory Lipkind for help in figure preparation and Megan McNulty for editorial assistance. Supported by HL-RO1-065661.

References

Ackerman, M.J., I. Splawski, J.C. Makielski, D.J. Tester, M.L. Will, K.W. Timothy, M.T. Keating, G. Jones, M. Chadha, C.R. Burrow, J.C. Stephens, C. Xu, R. Judson, and M.E. Curran. 2004. Spectrum and prevalence of cardiac sodium channel variants among black, white, Asian, and Hispanic individuals: Implications for arrhythmogenic susceptibility and Brugada/long QT syndrome genetic testing. *Heart Rhythm* 1:600–607.

Aldrich, R.W., D.P. Corey, and C.F. Stevens. 1983. A reinterpretation of mammalian sodium channel gating based on single channel recording. *Nature* 306:436–441.

Aldrich, R.W., and C.F. Stevens. 1987. Voltage-dependent gating of single sodium channels from mammalian neuroblastoma cells. *J. Neurosci*. 7:418–431.

Armstrong, C.M., and F. Bezanilla. 1977. Inactivation of the sodium channel. II. Gating current experiments. *J. Gen. Physiol*. 70:567–590.

Backx, P.H., D.T. Yue, J.H. Lawrence, E. Marban, and G.F. Tomaselli. 1992. Molecular localization of an ion-binding site within the pore of mammalian sodium channels. *Science* 257:248–251.

Balser, J.R., H.B. Nuss, N. Chiamvimonvat, M.T. Perez-Garcia, E. Marban, and G.F. Tomaselli. 1996. External pore residue mediates slow inactivation in mu 1 rat skeletal muscle sodium channels. *J. Physiol*. 494(Pt 2):431–442.

Barchi, R.L. 1997. Ion channel mutations and diseases of skeletal muscle. *Neurobiol. Dis*. 4:254–264.

Becker, S., E. Prusak-Sochaczewski, G. Zamponi, A.G. Beck-Sickinger, R.D. Gordon, and R.J. French. 1992. Action of derivatives of mu-conotoxin GIIIA on sodium channels. Single amino acid substitutions in the toxin separately affect association and dissociation rates. *Biochemistry* 31:8229–8238.

Benitah, J.P., Z. Chen, J.R. Balser, G.F. Tomaselli, and E. Marban. 1999. Molecular dynamics of the sodium channel pore vary with gating: Interactions between P-segment motions and inactivation. *J. Neurosci*. 19:1577–1585.

Berman, M.F., J.S. Camardo, R.B. Robinson, and S.A. Siegelbaum. 1989. Single sodium channels from canine ventricular myocytes: Voltage dependence and relative rates of activation and inactivation. *J. Physiol*. 415:503–531.

Bezanilla, F. 2000. The voltage sensor in voltage-dependent ion channels. *Physiol. Rev*. 80:555–592.

Cannon, S.C. 1996. Ion-channel defects and aberrant excitability in myotonia and periodic paralysis. *Trends Neurosci*. 19:3–10.

Cannon, S.C. 2000. Spectrum of sodium channel disturbances in the nondystrophic myotonias and periodic paralyses. *Kidney Int*. 57:772–779.

Catterall, W.A. 1980. Neurotoxins that act on voltage-sensitive sodium channels in excitable membranes. *Annu. Rev. Pharmacol. Toxicol*. 20:15–43.

Catterall, W.A. 2000. From ionic currents to molecular mechanisms: The structure and function of voltage-gated sodium channels. *Neuron* 26:13–25.

Chang, N.S., R.J. French, G.M. Lipkind, H.A. Fozzard, and S. Dudley Jr. 1998. Predominant interactions between mu-conotoxin Arg-13 and the skeletal muscle Na^+ channel localized by mutant cycle analysis. *Biochemistry* 37:4407–4419.

Chen, Q., G.E. Kirsch, D. Zhang, R. Brugada, J. Brugada, P. Brugada, D. Potenza, A. Moya, M. Borggrefe, G. Breithardt, R. Ortiz-Lopez, Z. Wang, C. Antzelevitch, R.E. O'Brien, E. Schulze-Bahr, M.T. Keating, J.A. Towbin, and Q. Wang. 1998. Genetic basis and molecular mechanism for idiopathic ventricular fibrillation. *Nature* 392:293–296.

Cummins, T.R., and F.J. Sigworth. 1996. Impaired slow inactivation in mutant sodium channels. *Biophys. J*. 71:227–236.

Doyle, D.A., J. Morais Cabral, R.A. Pfuetzner, A. Kuo, J.M. Gulbis, S.L. Cohen, B.T. Chait, and R. MacKinnon. 1998. The structure of the potassium channel: Molecular basis of K^+ conduction and selectivity. *Science* 280:69–77.

Dudley, S.C., Jr., N. Chang, J. Hall, G. Lipkind, H.A. Fozzard, and R.J. French. 2000. mu-conotoxin GIIIA interactions with the voltage-gated Na(+) channel predict a clockwise arrangement of the domains. *J. Gen. Physiol*. 116:679–690.

Favre, I., E. Moczydlowski, and L. Schild. 1996. On the structural basis for ionic selectivity among Na^+, K^+, and Ca^{2+} in the voltage-gated sodium channel. *Biophys. J*. 71:3110–3125.

Featherstone, D.E., J.E. Richmond, and P.C. Ruben. 1996. Interaction between fast and slow inactivation in Skm1 sodium channels. *Biophys. J*. 71:3098–3109.

Fozzard, H.A., and D.A. Hanck. 1996. Structure and function of voltage-dependent sodium channels: Comparison of brain II and cardiac isoforms. *Physiol. Rev*. 76:887–926.

French, R.J., and S.C. Dudley Jr. 1999. Pore-blocking toxins as probes of voltage-dependent channels. *Methods Enzymol*. 294:575–605.

Goldin, A.L. 2001. Resurgence of sodium channel research. *Annu. Rev. Physiol*. 63:871–894.

Guy, H.R., and P. Seetharamulu. 1986. Molecular model of the action potential sodium channel. *Proc. Natl. Acad. Sci. USA* 83:508–512.

Hanck, D.A., and M.F. Sheets. 1995. Modification of inactivation in cardiac sodium channels: Ionic current studies with Anthopleurin-A toxin. *J. Gen. Physiol*. 106:601–616.

Hanck, D.A., M.F. Sheets, and H.A. Fozzard. 1990. Gating currents associated with Na channels in canine cardiac Purkinje cells. *J. Gen. Physiol*. 95:439–457.

Heinemann, S.H., H. Terlau, and K. Imoto. 1992. Molecular basis for pharmacological differences between brain and cardiac sodium channels. *Pflugers Arch*. 422:90–92.

Hilber, K., W. Sandtner, O. Kudlacek, I.W. Glaaser, E. Weisz, J.W. Kyle, R.J. French, H.A. Fozzard, S.C. Dudley, and H. Todt. 2001. The selectivity filter of the voltage-gated sodium channel is involved in channel activation. *J. Biol. Chem*. 276:27831–27839.

Hilber, K., W. Sandtner, T. Zarrabi, E. Zebedin, O. Kudlacek, H.A. Fozzard, and H. Todt. 2005. Selectivity filter residues contribute unequally to pore stabilization in voltage-gated sodium channels. *Biochemistry* 44:13874–13882.

Hodgkin, A.L., and A.F. Huxley. 1952. A quantitative description of membrane current and its application to conduction and excitation in nerve. *J. Physiol*. 117:500–544.

Hoshi, T., W.N. Zagotta, and R.W. Aldrich. 1990. Biophysical and molecular mechanisms of Shaker potassium channel inactivation. *Science* 250:533–538.

Hui, K., G. Lipkind, H.A. Fozzard, and R.J. French. 2002. Electrostatic and steric contributions to block of the skeletal muscle sodium channel by mu-conotoxin. *J. Gen. Physiol*. 119:45–54.

Jiang, Y., A. Lee, J. Chen, M. Cadene, B.T. Chait, and R. MacKinnon. 2002. Crystal structure and mechanism of a calcium-gated potassium channel. *Nature* 417:515–522.

Khan, A., L. Romantseva, A. Lam, G. Lipkind, and H.A. Fozzard. 2002. Role of outer ring carboxylates of the rat skeletal muscle sodium channel pore in proton block. *J. Physiol*. 543:71–84.

Kuroda, Y., K. Miyamoto, M. Matsumoto, Y. Maeda, K. Kanaori, A. Otaka, N. Fujii, and T. Nakagawa. 2000. Structural study of the sodium channel inactivation gate peptide including an isoleucine–phenylalanine–methionine motif and its analogous peptide (phenylalanine/glutamine) in trifluoroethanol solutions and SDS micelles. *J. Pept. Res*. 56:172–184.

Lipkind, G.M., and H.A. Fozzard. 1994. A structural model of the tetrodotoxin and saxitoxin binding site of the Na^+ channel. *Biophys. J*. 66:1–13.

Lipkind, G.M., and H.A. Fozzard. 2000. KcsA crystal structure as framework for a molecular model of the Na(+) channel pore. *Biochemistry* 39:8161–8170.

Lipkind, G.M., and H.A. Fozzard. 2005. Molecular modeling of local anesthetic drug binding by voltage-gated sodium channels. *Mol. Pharmacol*. 68:1611–1622.

Makielski, J.C., M.F. Sheets, D.A. Hanck, C.T. January, and H.A. Fozzard. 1987. Sodium current in voltage clamped internally perfused canine cardiac Purkinje cells. *Biophys. J*. 52:1–11.

Makielski, J.C., B. Ye, C.R. Valdivia, M.D. Pagel, J. Pu, D.J. Tester, and M.J. Ackerman. 2003. A ubiquitous splice variant and a common polymorphism affect heterologous expression of recombinant human SCN5A heart sodium channels. *Circ. Res*. 93:821–828.

Noda, M., H. Suzuki, S. Numa, and W. Stuhmer. 1989. A single point mutation confers tetrodotoxin and saxitoxin insensitivity on the sodium channel II. *FEBS Lett*. 259:213–216.

Ong, B.H., G.F. Tomaselli, and J.R. Balser. 2000. A structural rearrangement in the sodium channel pore linked to slow inactivation and use dependence. *J. Gen. Physiol*. 116:653–662.

O'Reilly, J.P., S.Y. Wang, R.G. Kallen, and G.K. Wang. 1999. Comparison of slow inactivation in human heart and rat skeletal muscle Na^+ channel chimaeras. *J. Physiol*. 515(Pt 1):61–73.

Penzotti, J.L., G. Lipkind, H.A. Fozzard, and S.C. Dudley Jr. 2001. Specific neosaxitoxin interactions with the Na^+ channel outer vestibule determined by mutant cycle analysis. *Biophys. J*. 80:698–706.

Ren, D., B. Navarro, H. Xu, L. Yue, Q. Shi, and D.E. Clapham. 2001. A prokaryotic voltage-gated sodium channel. *Science* 294:2372–2375.

Richmond, J.E., D.E. Featherstone, H.A. Hartmann, and P.C. Ruben. 1998. Slow inactivation in human cardiac sodium channels. *Biophys. J*. 74:2945–2952.

Rohl, C.A., F.A. Boeckman, C. Baker, T. Scheuer, W.A. Catterall, and R.E. Klevit. 1999. Solution structure of the sodium channel inactivation gate. *Biochemistry* 38:855–861.

Rudy, B. 1978. Slow inactivation of the sodium conductance in squid giant axons. Pronase resistance. *J. Physiol*. 283:1–21.

Sandtner, W., J. Szendroedi, T. Zarrabi, E. Zebedin, K. Hilber, I. Glaaser, H.A. Fozzard, S.C. Dudley, and H. Todt. 2004. Lidocaine: A foot in the door of the inner vestibule prevents ultra-slow inactivation of a voltage-gated sodium channel. *Mol. Pharmacol*. 66:648–657.

Satin, J., J.W. Kyle, M. Chen, P. Bell, L.L. Cribbs, H.A. Fozzard, and R.B. Rogart. 1992. A mutant of TTX-resistant cardiac sodium channels with TTX-sensitive properties. *Science* 256:1202–1205.

Scanley, B.E., D.A. Hanck, T. Chay, and H.A. Fozzard. 1990. Kinetic analysis of single sodium channels from canine cardiac Purkinje cells. *J. Gen. Physiol*. 95:411–437.

Schild, L., and E. Moczydlowski. 1994. Permeation of Na^+ through open and Zn(2+)-occupied conductance states of cardiac sodium channels modified by batrachotoxin: Exploring ion–ion interactions in a multi-ion channel. *Biophys. J*. 66:654–666.

Schlief, T., R. Schonherr, K. Imoto, and S.H. Heinemann. 1996. Pore properties of rat brain II sodium channels mutated in the selectivity filter domain. *Eur. Biophys. J*. 25:75–91.

Sheets, M.F., and D.A. Hanck. 1995. Voltage-dependent open-state inactivation of cardiac sodium channels: Gating current studies with Anthopleurin-A toxin. *J. Gen. Physiol*. 106:617–640.

Sheets, M.F., and D.A. Hanck. 1999. Gating of skeletal and cardiac muscle sodium channels in mammalian cells. *J. Physiol*. 514(Pt 2):425–436.

Sheets, M.F., and D.A. Hanck. 2003. Molecular action of lidocaine on the voltage sensors of sodium channels. *J. Gen. Physiol*. 121:163–175.

Sheets, M.F., and D.A. Hanck. 2005. Charge immobilization of the voltage sensor in domain IV is independent of sodium current inactivation. *J. Physiol*. 563:83–93.

Sheets, M.F., J.W. Kyle, and D.A. Hanck. 2000. The role of the putative inactivation lid in sodium channel gating current immobilization. *J. Gen. Physiol*. 115:609–620.

Sheets, M.F., J.W. Kyle, R.G. Kallen, and D.A. Hanck. 1999. The Na channel voltage sensor associated with inactivation is localized to the external charged residues of domain IV, S4. *Biophys. J*. 77:747–757.

Splawski, I., K.W. Timothy, M. Tateyama, C.E. Clancy, A. Malhotra, A.H. Beggs, F.P. Cappuccio, G.A. Sagnella, R.S. Kass, and M.T. Keating. 2002. Variant of SCN5A sodium channel implicated in risk of cardiac arrhythmia. *Science* 297:1333–1336.

Struyk, A.F., and S.C. Cannon. 2002. Slow inactivation does not block the aqueous accessibility to the outer pore of voltage-gated Na channels. *J. Gen. Physiol*. 120:509–516.

Stuhmer, W., F. Conti, H. Suzuki, X.D. Wang, M. Noda, N. Yahagi, H. Kubo, and S. Numa. 1989. Structural parts involved in activation and inactivation of the sodium channel. *Nature* 339:597–603.

Sunami, A., A. Tracey, I.W. Glaaser, G.M. Lipkind, D.A. Hanck, and H.A. Fozzard. 2004. Accessibility of mid-segment domain IV S6 residues of the voltage-gated Na^+ channel to methanethiosulfonate reagents. *J. Physiol*. 561:403–413.

Terlau, H., S.H. Heinemann, W. Stuhmer, M. Pusch, F. Conti, K. Imoto, and S. Numa. 1991. Mapping the site of block by tetrodotoxin and saxitoxin of sodium channel II. *FEBS Lett*. 293:93–96.

Todt, H., S.C. Dudley Jr., J.W. Kyle, R.J. French, and H.A. Fozzard. 1999. Ultra-slow inactivation in mu1 Na^+ channels is produced by a structural rearrangement of the outer vestibule. *Biophys. J*. 76:1335–1345.

Townsend, C., and R. Horn. 1997. Effect of alkali metal cations on slow inactivation of cardiac Na^+ channels. *J. Gen. Physiol*. 110:23–33.

Ulbricht, W. 2005. Sodium channel inactivation: Molecular determinants and modulation. *Physiol. Rev*. 85:1271–1301.

Vandenberg, C.A., and F. Bezanilla. 1991. Single-channel, macroscopic, and gating currents from sodium channels in the squid giant axon. *Biophys. J*. 60:1499–1510.

Vedantham, V., and S.C. Cannon. 1998. Slow inactivation does not affect movement of the fast inactivation gate in voltage-gated Na^+ channels. *J. Gen. Physiol*. 111:83–93.

Vedantham, V., and S.C. Cannon. 1999. The position of the fast-inactivation gate during lidocaine block of voltage-gated Na^+ channels. *J. Gen. Physiol*. 113:7–16.

Vedantham, V., and S.C. Cannon. 2000. Rapid and slow voltage-dependent conformational changes in segment IVS6 of voltage-gated Na(+) channels. *Biophys. J*. 78:2943–2958.

Wallace, R.H., D.W. Wang, R. Singh, I.E. Scheffer, A.L. George Jr., H.A. Phillips, K. Saar, A. Reis, E.W. Johnson, G.R. Sutherland, S.F. Berkovic, and J.C. Mulley. 1998. Febrile seizures and generalized epilepsy associated with a mutation in the Na^+-channel beta1 subunit gene SCN1B. *Nat. Genet*. 19:366–370.

Wang, Q., J. Shen, I. Splawski, D. Atkinson, Z. Li, J.L. Robinson, A.J. Moss, J.A. Towbin, and M.T. Keating. 1995. SCN5A mutations associated with an inherited cardiac arrhythmia, long QT syndrome. *Cell* 80:805–811.

West, J.W., D.E. Patton, T. Scheuer, Y. Wang, A.L. Goldin, and W.A. Catterall. 1992. A cluster of hydrophobic amino acid residues required for fast Na(+)-channel inactivation. *Proc. Natl. Acad. Sci. USA* 89:10910–10914.

Xiong, W., R.A. Li, Y. Tian, and G.F. Tomaselli. 2003. Molecular motions of the outer ring of charge of the sodium channel: Do they couple to slow inactivation? *J. Gen. Physiol*. 122:323–332.

Yarov-Yarovoy, V., J.C. McPhee, D. Idsvoog, C. Pate, T. Scheuer, and W.A. Catterall. 2002. Role of amino acid residues in transmembrane segments IS6 and IIS6 of the Na^+ channel alpha subunit in voltage-dependent gating and drug block. *J. Biol. Chem*. 277:35393–35401.

Yue, D.T., J.H. Lawrence, and E. Marban. 1989. Two molecular transitions influence cardiac sodium channel gating. *Science* 244:349–352.